A Study on the Structures of 3-Methoxycarbonylrifamycins † by *X*-Ray Crystallography and ^{1}H Nuclear Magnetic Resonance Spectroscopy

Luciano Cellai, Silvio Cerrini,* and Annalaura Segre
Istituto di Strutturistica Chimica ' Giordano Giacomello ', C.N.R., C.P.10, 00016 Monterotondo Stazione, Rome, Italy
Mario Brufani
Gruppo di Chimica Biologica e Strutturistica Chimica, University of Rome, 00100 Rome, Italy
Walter Fedeli
Istituto di Chimica Farmaceutica e Tossicologica, University of Bologna, 40126 Bologna, Italy
Alessandro Vaciago
Chemical Crystallography Laboratory, University of Oxford, Oxford OX1 3PD

The structures of 3-methoxycarbonylrifamycins † were studied by *X*-ray crystallography and ^{1}H n.m.r. spectroscopy. The results obtained by the two different methods are consistent. The comparison with the conformations of some ansamycins in the solid state shows that in this and in other active compounds the central part of the *ansa*-chain, directly involved in the inhibitory interaction with the bacterial enzyme DNA-dependent RNA polymerase, remains in general the same, while large conformational changes may occur at the junctions of the *ansa*-chain with the chromophore-rings, thus generating four kinds of conformers. Therefore the 3-methoxycarbonyl substituent does not seem to exert any influence on the conformation of the *ansa*-chain which can be related to the decrease of the antibacterial activity of 3-methoxycarbonylrifamycin S.

Rifamycins, a class of natural and semisynthetic antibiotics belonging to the family of ansamycins, are well known inhibitors of bacterial DNA-dependent RNA polymerase.[1,2]

A structure–activity study on the influence of 3-substituents in rifamycin S (I) (and SV), led to the synthesis of 3-carboxyrifamycin S and a series of derivatives, and to the testing of their antimicrobial activity, which unexpectedly turned out to be rather low.[3] This finding prompted us to undertake the determination of the crystal structure of one of these compounds, in order to verify if an inactivating conformational variation had occurred that could be attributed to the introduction of the 3-methoxycarbonyl group. Therefore, the crystal structure of 3-methoxycarbonylrifamycin S (CMRS) (II) was determined by *X*-ray diffraction; its conformation was also studied in solution by ^{1}H n.m.r., and it was compared with the known structures of other naphthylansamycins, *i.e.* rifamycin B *p*-iodoanilide[4] (RIFB) (III; R^2 = CH_2-$CONHC_6H_4I$), rifampicin[5] (RIFMP) (IV), tolypomycinone tris-*m*-bromobenzoate[6] (BRTOL) (V), and tolypomycinone[7] (TOL) (VI). The results of these experiments are presented in this paper.

Experimental

Crystal Structure Determination.—Well shaped, red crystals of 3-methoxycarbonylrifamycin S (II) were grown from a water–ethanol solution at room temperature. They are monoclinic, $C_{39}H_{47}NO_{14}\cdot H_2O$, *M* 721.823, *a* = 13.610 ± 0.005, *b* = 15.845 ± 0.007, *c* = 10.129 ± 0.004 Å, β = 113.37 ± 0.03°, *U* = 2 005 Å^3, D_c = 1.278, *Z* = 2, *F*(000) = 820. Space group $P2_1$ (C_2^2 No. 4) from systematic absences; Mo-K_α radiation, λ = 0.710 69 Å, μ(Mo-K_α) = 1.06 cm^{-1}, crystal dimensions 0.4 × 0.5 × 0.7 mm. The unit cell parameters were determined by least-squares calculation of the 2θ values of 15 selected reflections. Intensities were collected at room temperature by the ω-scan technique up to sin θ/λ = 0.64. Data were recorded with a scan rate between 0.5 and 29.0° min^{-1}, depending on the intensity, and with a scan range of 1.0° centred on the calculated Bragg scattering angle. Periodic checks of the intensity values of four standard reflections did not reveal any significant *X*-ray damage or crystal decay. Estimated standard deviations of the intensities were based on counting statistics. From among the 4 526 measured diffraction data, 3 363 unique reflections with $F_0^2 > 2\sigma(F_0^2)$ were selected as observed structure amplitudes.

The crystal structure was solved by a combination of direct methods and conventional Fourier procedure. Indeed, the MULTAN 76 program,[8] applied to 500 reflections with the highest |*E*(*hkl*)| values, and processing 5 000 Σ_2 relationships revealed, in an *E* map calculated with one of the best sets of phases, only a significant molecular fragment of 26 peaks corresponding mainly to the naphthoquinone nucleus. The first structure factor calculation based on this model, assuming a carbon form factor and *B* = 3 Å^2 for all the atoms, gave *R* 0.44. From among the peaks of the subsequent Fourier synthesis, only eight, those corresponding to the peaks of the previous *E* map, were accepted as new atomic positions and a structure factor calculation gave *R* 0.42. Cyclic iterations of structure factors, least-squares, and Fourier synthesis calculations allowed the remaining atoms and the water solvent molecule to be localised. The crystal structure was refined by block-diagonal (9 × 9) least-squares calculations up to *R* 0.072 with anisotropic temperature factors for all the non-hydrogen atoms. All the 49 hydrogens were then found by difference Fourier synthesis, using only data with sin θ/λ ≤ 0.5. Refinement was ended by a few least-squares calculations using anisotropic temperature factors for the non-hydrogen atoms while for the hydrogens all the parameters were kept fixed, with *B* values equal to those of the carrier atoms. The final *R* value is 0.047. The refinement was accomplished by

† Both at the 3rd Meeting of the Italian and Jugoslavian Crystallographic Associations, Parma, 1979, and at the 5th European Crystallographic Meeting, Copenhagen, 1979, a paper was presented by us on the supposed structure of 3-methoxycarbonylrifamycin SV, such as would have been expected on the basis of the chemical preparation. A further refinement of the data revealed that the structure of 3-methoxycarbonylrifamycin S had been determined instead, an oxidation of the naphthohydroquinone nucleus having occurred during crystallization.

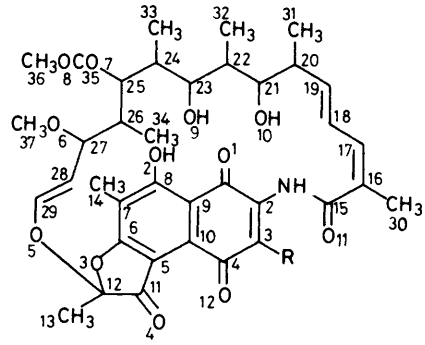

(I) R = H
(II) R = $COOCH_3$

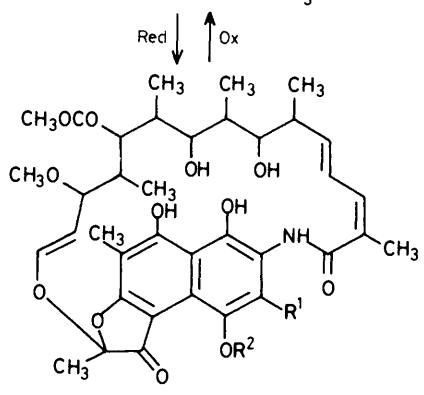

(III) R^1 = H; R^2 = CH_2COOH

(IV) R^1 = CH=N—N N—CH_3; R^2 = H

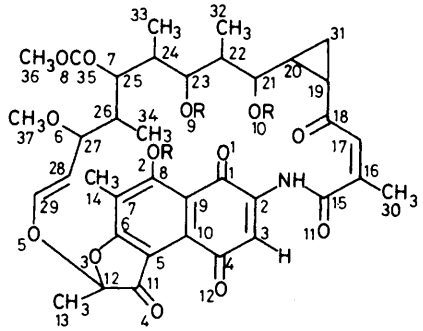

(V) R = CO—C6H4—Br
(VI) R = H

assigning to each reflection the weight $w = (a + |F_0| + c|F_0|^2)^{-1}$ with $a = 8.8$ and $c = 0.0084$ selected to get a relatively constant average $\langle w|\Delta F|^2\rangle$ in groups of F_0 and sin θ/λ.[9] The atomic scattering factors were taken from literature.[10] The calculations were carried out on the Univac 1110 computer of Rome University and on the H.P. 2100 minicomputer of the C.N.R. Research Area, Rome, and were performed by a system of programs developed in this laboratory.[11,12]

The atomic co-ordinates * of CMRS (II) are listed in Table 1 and define, in a right-handed system, the absolute configuration of the molecule according to that of Leitich *et al.*[13] The molecular structure of CMRS (II) is represented in Figure 1, which shows the similarity of CMRS with the other

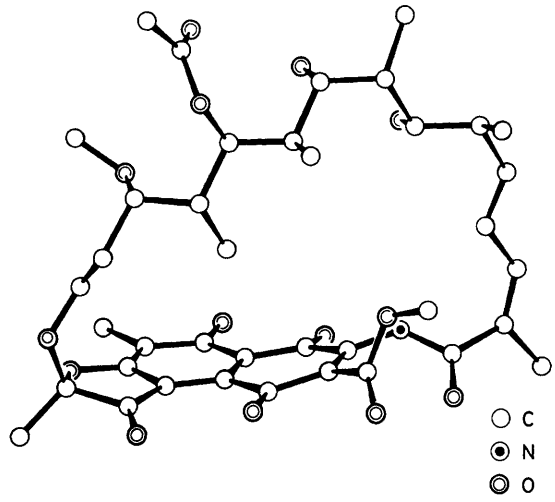

Figure 1. Molecular structure of CMRS (II) (non-hydrogen atoms only)

ansamycins together with some conformational peculiarities, concerning both the amide group and the double bond C(27)=C(28), which will be discussed later. Bond lengths and angles for the heavy atoms are given in Tables 2 and 3, respectively.

For the hydrogens, the mean distances from the parent atoms are d(C–H) = 0.99(8), d(O–H) = 0.98(1), d(N–H) = 0.88(6) Å while the average values of the bond angles are 109(8), 117(4), 115(3), and 109(5)° for C(sp^3), C(sp^2), N, and O carrier atoms, respectively. Intramolecular hydrogen bonds occur between O(1) and O(2) (2.54 Å), O(8) and O(9) (2.89 Å), and O(9) and O(10) (2.72 Å) with O(1), O(8), and O(9) as acceptors. Each water (solvent) molecule is involved as a donor in two intermolecular hydrogen bonds, O(15)–O(10) (2.89 Å) and O(15)–O(13) (2.92 Å), where O(10) and O(13) belong to different molecules related by a screw axis as shown in Figure 2.

^{1}H *N.m.r. Analysis.*—^{1}H N.m.r. spectra for CMRS (II) and CMRSV (hydroquinone form of CMRS) were obtained at 400, 270, and 200 MHz in $CDCl_3$, CD_2Cl_2, and D_2O. The 400 MHz spectrum of CMRSV in $CDCl_3$ at 21 °C is rather broad and does not allow signal assignment; at 270 MHz some lines are sharper than others; at 200 MHz most lines are quite sharp. Low-temperature (−58 °C) spectra at 270 MHz in $CDCl_3$ show that some splitting occurs; however, resonances are still too broad to be assigned. This behaviour can be interpreted as due to the existence of more than one conformer in solution and will be discussed in a separate paper.[14] Our results indicate that many derivatives of rifamycin SV show the same behaviour in organic solvents.

The 400 MHz spectrum of CMRSV in D_2O is very sharp; thus all peaks were assigned by systematic spin decoupling. It cannot be ruled out that also in D_2O two conformations exist, but rapidly interconvert. Chemical shifts and coupling constants are set out in Table 4. From this assignment an optimized Karplus-type [15] analysis was performed leading to H–C–C–H torsion angles as set out in Table 5. It was also found that the carbonyl group is reversed with respect to the

* The observed amplitudes, calculated structure factors, and atomic thermal parameters are in Supplementary Publication No. SUP 23406 (25 pp.). For details of Supplementary Publications see Notice to Authors No. 7 in *J. Chem. Soc., Perkin Trans. 2*, 1981, Index issue.

Table 1. Fractional atomic co-ordinates with their estimated standard deviations (e.s.d.s in parentheses)

Atom	*x/a*	*y/b*	*z/c*
C(1)	0.322 2(3)	0.2141	0.959 0(4)
C(2)	0.427 6(3)	0.230 1(3)	0.946 4(4)
C(3)	0.433 6(3)	0.285 9(3)	0.849 9(4)
C(4)	0.337 6(3)	0.332 7(3)	0.751 8(4)
C(5)	0.133 9(4)	0.336 6(3)	0.642 7(4)
C(6)	0.038 0(3)	0.303 0(3)	0.637 3(4)
C(7)	0.027 9(3)	0.247 1(3)	0.735 1(5)
C(8)	0.124 5(3)	0.221 9(3)	0.843 8(4)
C(9)	0.225 8(3)	0.250 0(3)	0.849 2(4)
C(10)	0.231 0(3)	0.308 4(3)	0.748 5(4)
C(11)	0.105 1(4)	0.396 3(3)	0.518 5(4)
C(12)	−0.016 6(4)	0.380 5(4)	0.431 4(5)
C(13)	−0.077 5(4)	0.212 6(4)	0.730 0(6)
C(14)	−0.084 3(5)	0.460 0(4)	0.386 9(6)
C(15)	0.612 7(3)	0.206 4(3)	1.116 9(4)
C(16)	0.682 2(3)	0.141 9(3)	1.217 6(4)
C(17)	0.703 1(3)	0.069 3(3)	1.174 1(5)
C(18)	0.667 9(4)	0.038 3(3)	1.026 0(5)
C(19)	0.707 2(4)	−0.031 5(3)	0.991 2(5)
C(20)	0.680 2(4)	−0.069 5(3)	0.846 4(5)
C(21)	0.564 3(4)	−0.051 4(3)	0.741 4(5)
C(22)	0.532 5(4)	−0.089 0(3)	0.591 0(5)
C(23)	0.418 6(4)	−0.068 1(3)	0.487 6(5)
C(24)	0.393 7(3)	0.027 2(2)	0.465 2(4)
C(25)	0.276 2(3)	0.043 4(2)	0.373 3(4)
C(26)	0.238 4(3)	0.135 1(3)	0.367 7(5)
C(27)	0.119 2(3)	0.141 9(3)	0.272 8(4)
C(28)	0.076 9(4)	0.231 8(3)	0.261 7(5)
C(29)	0.012 3(4)	0.255 6(3)	0.321 7(5)
C(30)	0.729 9(5)	0.170 5(4)	1.372 9(5)
C(31)	0.760 9(5)	−0.040 6(6)	0.785 5(7)
C(32)	0.549 1(6)	−0.186 3(4)	0.595 0(6)
C(33)	0.467 7(4)	0.070 0(3)	0.405 4(6)
C(34)	0.263 9(4)	0.167 8(4)	0.519 1(6)
C(35)	0.200 4(4)	−0.053 9(3)	0.174 2(5)
C(36)	0.168 9(6)	−0.062 3(5)	0.016 8(6)
C(37)	−0.029 7(5)	0.052 9(5)	0.217 2(9)
C(38)	0.534 8(3)	0.299 3(3)	0.827 7(4)
C(39)	0.670 5(5)	0.226 3(4)	0.781 8(8)
N	0.508 7(3)	0.181 4(3)	1.041 2(4)
O(1)	0.321 3(3)	0.172 5(3)	1.058 7(3)
O(2)	0.118 3(3)	0.166 7(3)	0.940 8(4)
O(3)	−0.051 2(2)	0.329 2(2)	0.523 1(3)
O(4)	0.153 5(3)	0.449 7(3)	0.486 1(4)
O(5)	−0.030 8(3)	0.335 9(3)	0.303 6(3)
O(6)	0.062 9(3)	0.085 5(2)	0.325 5(4)
O(7)	0.251 8(2)	0.019 1(2)	0.224 3(3)
O(8)	0.182 3(3)	−0.104 9(2)	0.251 4(4)
O(9)	0.345 9(3)	−0.108 9(2)	0.540 8(4)
O(10)	0.497 8(3)	−0.082 1(3)	0.810 4(4)
O(11)	0.643 2(3)	0.277 0(2)	1.106 0(4)
O(12)	0.346 1(3)	0.383 7(3)	0.667 5(5)
O(13)	0.576 6(3)	0.365 3(2)	0.825 2(4)
O(14)	0.568 5(3)	0.224 7(2)	0.797 1(4)
O(15)	0.426 9(4)	0.011 7(3)	1.001 2(6)
H(1)	0.0731	0.7179	0.1648
H(2)	0.0818	0.6480	0.2996
H(3)	0.1284	0.7359	0.3351
H(4)	0.1756	0.9361	0.6792
H(5)	0.0873	0.9867	0.5223
H(6)	0.0728	0.9948	0.6830
H(7)	0.2535	0.5314	0.7669
H(8)	0.3844	0.5774	0.0600
H(9)	0.2471	0.4391	0.9336
H(10)	0.3249	0.3740	0.1269
H(11)	0.4376	0.5134	0.2591
H(12)	0.4239	0.4361	0.4556
H(13)	0.4212	0.9106	0.4041
H(14)	0.4186	0.0491	0.5520
H(15)	0.2336	0.0128	0.4113
H(16)	0.2914	0.1706	0.3308
H(17)	0.0958	0.1271	0.1712
H(18)	0.1013	0.2657	0.2169
H(19)	0.0208	0.7087	0.6443
H(20)	0.2361	0.7252	0.6350
H(21)	0.3170	0.6834	0.5750
H(22)	0.2257	0.6142	0.5690
H(23)	0.2369	0.4245	0.3156
H(24)	0.1623	0.4611	0.1264
H(25)	0.2606	0.5208	0.2322
H(26)	0.3753	0.3018	0.3630
H(27)	0.4769	0.2942	0.3652
H(28)	0.4784	0.2904	0.4889
H(29)	0.4553	0.1181	0.3893
H(30)	0.4472	0.0374	0.2995
H(31)	0.4661	0.5646	0.5245
H(32)	0.2263	0.1373	0.5704
H(33)	0.3448	0.1742	0.5823
H(34)	0.2188	0.2118	0.5099
H(35)	0.1575	0.8896	1.0125
H(36)	0.2370	0.9615	1.0112
H(37)	0.1071	0.9721	0.9870
H(38)	0.0516	0.5174	0.7337
H(39)	0.0236	0.5032	0.8623
H(40)	0.0642	0.5956	0.8099
H(41)	0.3285	0.6734	0.2365
H(42)	0.2785	0.7397	0.1114
H(43)	0.3434	0.7649	0.3303
H(44)	0.4895	0.1390	0.0815
H(45)	0.1866	0.1645	1.0113
H(46)	0.2720	0.8887	0.4630
H(47)	0.4459	0.8975	0.7607
H(48)	0.4280	−0.0371	1.0818
H(49)	0.4333	−0.0158	0.9330

Table 2. Bond lengths (Å) with e.s.d.s (in parentheses)

C(1)–C(2)	1.512(6)	C(17)–C(18)	1.466(8)
C(1)–C(9)	1.457(7)	C(18)–C(19)	1.337(7)
C(1)–O(1)	1.210(5)	C(19)–C(20)	1.490(8)
C(2)–C(3)	1.344(6)	C(20)–C(21)	1.540(9)
C(2)–N	1.376(7)	C(20)–C(31)	1.527(8)
C(3)–C(4)	1.488(8)	C(21)–C(22)	1.530(7)
C(3)–C(38)	1.497(6)	C(21)–O(10)	1.431(6)
C(4)–C(10)	1.488(7)	C(22)–C(23)	1.524(9)
C(4)–O(12)	1.215(6)	C(22)–C(32)	1.555(8)
C(5)–C(6)	1.390(7)	C(23)–C(24)	1.545(6)
C(5)–C(10)	1.404(8)	C(23)–O(9)	1.453(6)
C(5)–C(11)	1.497(7)	C(24)–C(25)	1.519(7)
C(6)–C(7)	1.376(7)	C(24)–C(33)	1.525(6)
C(6)–O(3)	1.368(7)	C(25)–C(26)	1.534(6)
C(7)–C(8)	1.397(8)	C(25)–O(7)	1.462(6)
C(7)–C(14)	1.518(8)	C(26)–C(27)	1.526(8)
C(8)–C(9)	1.428(6)	C(26)–C(34)	1.523(8)
C(8)–O(2)	1.343(6)	C(27)–C(28)	1.524(7)
C(9)–C(10)	1.400(6)	C(27)–O(6)	1.412(5)
C(11)–C(12)	1.557(9)	C(28)–C(29)	1.307(6)
C(11)–O(4)	1.196(7)	C(29)–O(5)	1.382(7)
C(12)–C(13)	1.520(9)	C(35)–C(36)	1.483(9)
C(12)–O(3)	1.447(6)	C(35)–O(7)	1.343(6)
C(12)–O(5)	1.419(6)	C(35)–O(8)	1.215(6)
C(15)–C(16)	1.487(8)	C(37)–O(6)	1.401(11)
C(15)–N	1.374(7)	C(38)–O(13)	1.195(6)
C(15)–O(11)	1.214(6)	C(38)–O(14)	1.347(6)
C(16)–C(17)	1.304(7)	C(39)–O(14)	1.456(7)
C(16)–C(30)	1.514(9)		

Table 3. Bond angles (°) with e.s.d.s (in parentheses)

C(2)–C(1)–C(9)	117.8(3)	C(15)–C(16)–C(30)	113.7(5)
C(2)–C(1)–O(1)	119.1(5)	C(17)–C(16)–C(30)	123.7(6)
C(9)–C(1)–O(1)	123.1(4)	C(16)–C(17)–C(18)	127.9(5)
C(1)–C(2)–C(3)	120.3(4)	C(17)–C(18)–C(19)	123.0(6)
C(1)–C(2)–N	111.9(3)	C(18)–C(19)–C(20)	128.8(6)
C(3)–C(2)–N	127.8(4)	C(19)–C(20)–C(21)	112.9(4)
C(2)–C(3)–C(4)	121.6(4)	C(19)–C(20)–C(31)	109.9(6)
C(2)–C(3)–C(38)	121.8(5)	C(21)–C(20)–C(31)	111.7(5)
C(4)–C(3)–C(38)	116.5(4)	C(20)–C(21)–C(22)	115.0(4)
C(3)–C(4)–C(10)	118.4(4)	C(20)–C(21)–O(10)	105.9(4)
C(3)–C(4)–O(12)	119.9(5)	C(22)–C(21)–O(10)	111.7(5)
C(10)–C(4)–O(12)	121.4(5)	C(21)–C(22)–C(23)	114.1(4)
C(6)–C(5)–C(10)	119.6(4)	C(21)–C(22)–C(32)	112.3(5)
C(6)–C(5)–C(11)	106.3(5)	C(23)–C(22)–C(32)	109.3(5)
C(10)–C(5)–C(11)	134.1(5)	C(22)–C(23)–C(24)	114.7(4)
C(5)–C(6)–C(7)	125.3(5)	C(22)–C(23)–O(9)	107.8(4)
C(5)–C(6)–O(3)	115.0(4)	C(24)–C(23)–O(9)	110.3(4)
C(7)–C(6)–O(3)	119.7(4)	C(23)–C(24)–C(25)	111.8(4)
C(6)–C(7)–C(8)	114.8(4)	C(23)–C(24)–C(33)	110.7(4)
C(6)–C(7)–C(14)	124.8(5)	C(25)–C(24)–C(33)	112.4(4)
C(8)–C(7)–C(14)	120.4(5)	C(24)–C(25)–C(26)	116.0(4)
C(7)–C(8)–C(9)	122.3(4)	C(24)–C(25)–O(7)	109.9(3)
C(7)–C(8)–O(2)	116.7(4)	C(26)–C(25)–O(7)	106.0(4)
C(9)–C(8)–O(2)	121.0(5)	C(25)–C(26)–C(27)	110.3(4)
C(1)–C(9)–C(8)	118.1(4)	C(25)–C(26)–C(34)	110.2(5)
C(1)–C(9)–C(10)	121.6(4)	C(27)–C(26)–C(34)	111.8(4)
C(8)–C(9)–C(10)	120.3(5)	C(26)–C(27)–C(28)	112.9(4)
C(4)–C(10)–C(5)	123.3(4)	C(26)–C(27)–O(6)	108.6(4)
C(4)–C(10)–C(9)	119.1(5)	C(28)–C(27)–O(6)	111.9(4)
C(5)–C(10)–C(9)	117.5(4)	C(27)–C(28)–C(29)	122.7(4)
C(5)–C(11)–C(12)	103.8(4)	C(28)–C(29)–O(5)	122.2(5)
C(5)–C(11)–O(4)	133.6(6)	C(36)–C(35)–O(7)	111.6(5)
C(12)–C(11)–O(4)	122.4(6)	C(36)–C(35)–O(8)	125.9(6)
C(11)–C(12)–C(13)	114.7(5)	O(7)–C(35)–O(8)	122.5(5)
C(11)–C(12)–O(3)	105.7(4)	C(3)–C(38)–O(13)	127.0(4)
C(13)–C(12)–O(3)	110.0(4)	C(3)–C(38)–O(14)	109.1(4)
C(11)–C(12)–O(5)	109.0(4)	O(13)–C(38)–O(14)	123.7(4)
C(13)–C(12)–O(5)	107.2(5)	C(2)–N–C(15)	126.3(4)
O(3)–C(12)–O(5)	110.1(4)	C(6)–O(3)–C(12)	107.9(4)
C(16)–C(15)–N	114.8(4)	C(12)–O(5)–C(29)	116.2(4)
C(16)–C(15)–O(11)	123.3(5)	C(27)–O(6)–C(37)	113.1(5)
N–C(15)–O(11)	121.9(5)	C(25)–O(7)–C(35)	119.2(3)
C(15)–C(16)–C(17)	122.6(5)	C(38)–O(14)–C(39)	115.7(4)

usual position previously found [4,5] in most rifamycin derivatives, because of the low chemical shift of H(18). In fact the resonance multiplet due to H(18) can lie in two spectral regions (varying the solvent as well as the oxidation state), *i.e.* either between δ 6.4 and 6.5 or between δ 6.8 and 7.1. The δ 6.4—6.5 region corresponds to the chemical shift of the C(3)–H in methylbutadiene [16] and of H(18) in rifampicin.[17] The second range of chemical shifts (δ 6.8—7.1) can be explained as due to a deshielding effect owing to the anisotropic carbonyl when this group is rotated as shown in Figure 1. Further details on the behaviour of the chemical shift of the multiplet due to H(18) are discussed in a separate paper.[14] Finally the lack of long-range coupling between H(27) and H(29) eliminates the ambiguity in the Karplus relationship [18] for the torsion angle H(27)–C(27)–C(28)–H(28). This angle is also very similar to the corresponding angle found in the solid state for CMRS (II).

^{1}H N.m.r. spectra of CMRS (II) were run at 270 and 200 MHz in $CDCl_3$ solution. The spectrum shows a double set of lines; this has been interpreted as due to the existence of two conformers having different populations (3 : 1) (Figure 3). Almost all lines present small differences of chemical shift for all protons, apart from H(18) where the difference is larger. Chemical shifts and coupling constants for the major conformer are set out in Table 4. From this assignment an optimized Karplus-type analysis [15] was performed leading to H–C–C–H torsion angles (Table 5). The chemical shift of the multiplet due to H(18) is found at the usual value; [17] it is thus reasonable to assume that the position of the carbonyl, for the major conformer in $CDCl_3$, is similar to the steric disposition found in rifampicin (Figure 5). Finally the presence of a long-range coupling constant between H(27) and H(29) eliminates the ambiguity in the Karplus relationship between H(27) and H(28). Thus the angle H(27)–C(27)–C(28)–H(28) can be obtained as shown in Table 5; the value of this angle is very similar to the value of the corresponding angle found in the solid state for rifampicin.[5]

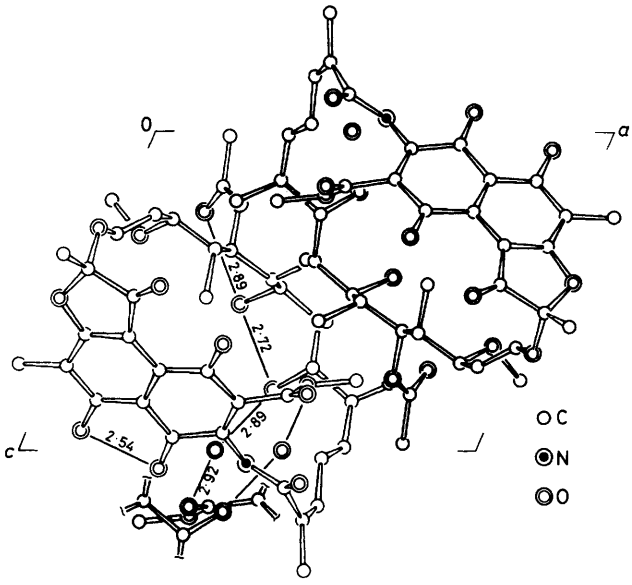

Figure 2. Crystal structure of CMRS (II) (non-hydrogen atoms only), projected along the *b* axis

^{1}H N.m.r. spectra of CMRS (II) were run at 270 and 200 MHz in D_2O solution; the spectra show a single set of lines.[3]

Results and Discussion

The molecular structure of CMRS (II), as determined by *X*-ray diffraction, is shown in Figure 1. The molecule displays an overall conformation resembling those of two active revealed, in an *E* map calculated with one of the best sets of rifamycins, rifamycin B *p*-iodoanilide [4] (III; $R^2 = CH_2$-$CONHC_6H_4I$), and rifampicin [5] (IV). Indeed, the least-squares plane containing the ten atoms of the chromophore rings, and that containing the seventeen atoms of the *ansa*-chain, make an angle of 97° in CMRS (II), which can be compared with the values 109 and 98° found for RIFB (III) and RIFMP (IV), respectively. Furthermore, the spatial arrangement of the four oxygens O(1), O(2), O(9), and O(10), supposed to be most relevant for biological activity, displays a common pattern in CMRS (II), RIFB (III), and RIFMP (IV). In fact, as can be seen by comparison of the molecular structure of CMRS (II) (Figure 1) with those of RIFB (III) (Figure 4) and RIFMP (IV) (Figure 5) and as illustrated in Tables 6 and 7, in all the three structures the O(9) and O(10) oxygens lie on the same side of O(1) and O(2) with respect to the best plane containing the *ansa*-chain, with bonds C(21)–O(10) and C(23)–O(9) nearly perpendicular to the plane. Besides these similarities, a comparison of the conformation of the seventeen-membered chain of CMRS (II) with those observed in the solid state for RIFB (III) and RIFMP (IV), as shown in Table 8, reveals that

Table 4. Chemical shifts (p.p.m. from Me_4Si) and coupling constants (Hz) along the *ansa*-chain of CMRS (II) and CMRSV. Experimental conditions: pulse angle 60°; sweep width 6 000 Hz at 400 MHz, otherwise 4 000 Hz; relaxation delay 3 s, 32 K memory. Experiments in D_2O were carried out with solvent suppression

CMRS in D_2O [3]		CMRS in $CDCl_3$ (major conformer)		CMRSV in D_2O			CMRSV in D_2O	CMRS in $CDCl_3$ (major conformer) [3]	CMRS in D_2O [3]
δ	*J*/Hz	δ	*J*/Hz	δ	*J*/Hz		δ	δ	δ
						C_{16}–CH_3	2.00	2.04	2.01
6.45		6.33		6.45		HC_{17}			
			10		11				
6.45		6.53		7.02		HC_{18}			
			16		16				
6.2		6.18		6.26		HC_{19}			
			7.5		7.5				
2.4		2.35		2.44		HC_{20}–CH_3	0.99	0.89	0.92
	11		10		9				
3.98		3.73		4.05		HC_{21}–OH		3.68 $J(H_{21}$–$OH_{21})$ 0	
	2.5—3		0		2				
		1.82		1.9		HC_{22}–CH_3	1.01	1.01	0.98
	2		2		2				
3.17		3.01		3.17		HC_{23}–OH		3.78 $J(H_{23}$–$OH_{23})$ 5	
	11		12		11				
1.4		1.7		1.47		HC_{24}–CH_3	0.71	0.70	0.75
			2.5		0				
5.2—5.3		4.81		5.10		HC_{25}–OAc	2.06	2.06	2.09
			11		11				
1.3		1.65		1.23		HC_{26}–CH_3	−0.23	0.20	0.15
	1—2		3		1				
3.57		3.43		3.55		HC_{27}–OMe	3.06	3.10	3.08
	5—6		8		7.5				
5.2—5.3		5.07		5.17		HC_{28}			
	12.5		12.5		13				
6.23		6.13		6.31		HC_{29}			

Table 5. H–C–C–H Torsion angles [15] (°) along the *ansa*-chain *

	CMRSV in D_2O	CMRS (II) in $CDCl_3$ majority conformer	CMRS (II) in D_2O
H(17)–H(18)	165	157	
H(19)–H(20)	32	33	
H(20)–H(21)	164	175	−175
H(21)–H(22)	57	66	60
H(22)–H(23)	52	52	65
H(23)–H(24)	−175	−175	−170
H(24)–H(25)	−80	−63	70
H(25)–H(26)	175	165	
H(26)–H(27)	69	53	
H(27)–H(28)	−33	138	−45

* The maximum error is 3° for angles in the range 0—70° and 110—180°; near 90° it is at least twice as large.

CMRS (II) undergoes conformational variations that occur only near the junctions of the *ansa*-chain with the chromophore rings, but which, nevertheless, leave the conformation of the central part of the *ansa*-chain almost unaffected. These variations occur on one side of the *ansa*-chain around the C(2)–N and C(15)–C(16) bonds and on the other side around the C(27)–C(28) and C(29)–O(5) bonds. In detail, in CMRS (II) the torsion angles around C(2)–N and C(15)–C(16) are −141 and 63°, respectively, while the corresponding values are −32 and −43° for RIFB (III), and −55 and −31° for RIFMP (IV). These two simultaneous rotations result in a reorientation of the amide group which is reversed with respect to that observed in the other two rifamycins. The amidic group is still antiperiplanar, while the carbonyl group turns from a +anticlinal to a −anticlinal conformation, with respect to the C(16)–C(17) double bond.

A similar conformation of this part of the *ansa*-chain has been observed in the molecular structure of other naphthyl ansamycins,* *i.e.* in tolypomycinone tris-*m*-bromobenzoate [6] (BRTOL) (V), and in tolypomycinone [7] (TOL) (VI) (Figure 6). The chromophoric nucleus is in the quinone form in CMRS

* The *X*-ray structures of rifamycin Y *p*-iodoanilide [4] and of rifamycin S iminomethyl ether [20] have not been considered in our discussion because the chemical modifications do not make them directly comparable with the other compounds.

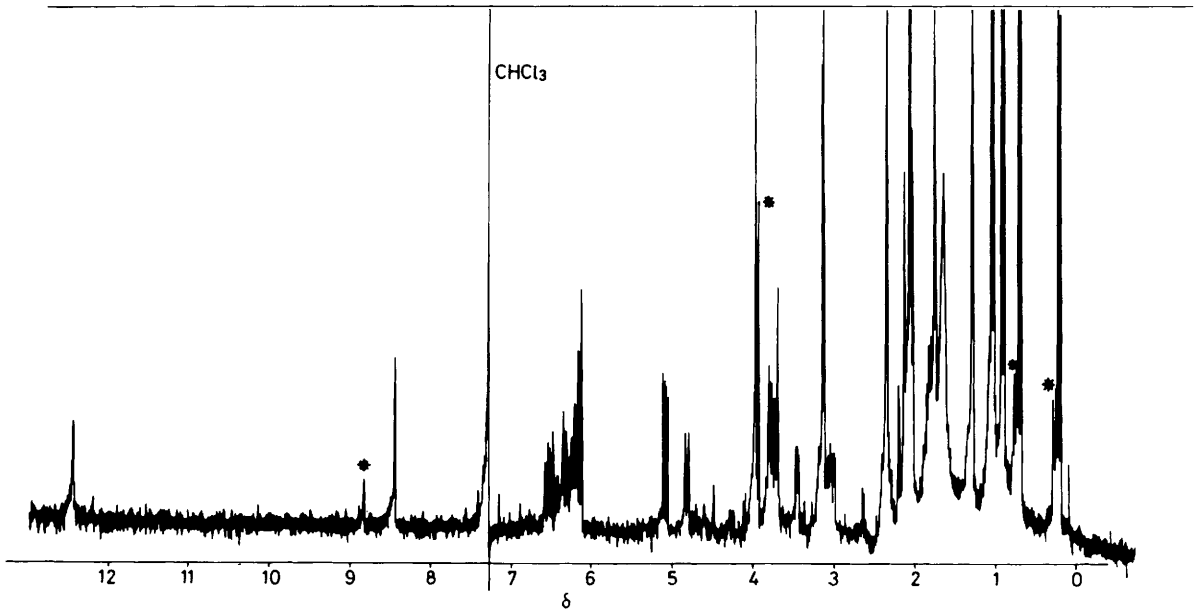

Figure 3. 270 MHz ^{1}H N.m.r. spectrum of CMRS (II) in $CDCl_3$ showing the presence of two conformers. * Indicates a resonance due to the minor conformer

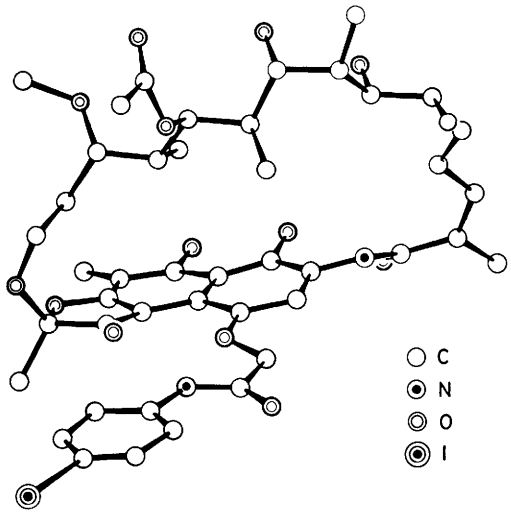

Figure 4. Molecular structure of RIFB (III) (in the same orientation as CMRS in Figure 1)

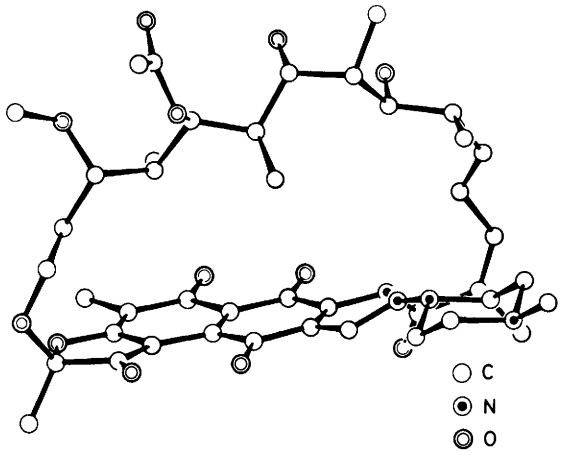

Figure 5. Molecular structure of RIFMP (IV) (in the same orientation as CMRS in Figure 1)

(II), BRTOL (V), and TOL (VI), while it is in the hydroquinone form in RIFB (III) and RIFMP (IV); furthermore a methoxycarbonyl substituent on C(3) is present in CMRS (II); this is *ortho* both to the quinone oxygen bound to C(4), and to the amide group bound to C(2); it is planar and makes an angle of 62° with the plane of the chromophore rings allowing O(13) and O(14) to assume roughly equal distances from O(11) and O(12): O(13)–O(11) = 2.970, O(13)–O(12) = 2.916, O(14)–O(11) = 2.998, and O(14)–O(12) = 3.752 Å.

The lack of coplanarity between the chromophore rings and the bulky methoxy-group might be due to steric hindrance. The second noteworthy conformational variation has been found on the other junction of the *ansa*-chain. In CMRS (II), in fact, the torsion angles along the bonds C(27)–C(28) and C(29)–O(5) are respectively −110 and −127° while they are 117 and 49° in RIFB (III), and 118 and 65° in RIFMP (IV). These two co-operative rotations lead the plane containing C(27), C(28), C(29), and O(5) to rotate around the O(5)–C(27) line, and to assume an opposite orientation. A similar conformation of this part of the *ansa*-chain has been observed, in the solid state, in BRTOL (V) (Figure 6), which is indeed the ansamycin of known crystal structure that more closely resembles CMRS (II), as shown in Figures 1, 6, and 7. Apart from the fragment between C(18) and C(20), which is chemically different, the remaining parts of the *ansa*-chains have conformational parameters very close to one another, with a root mean square difference of 12°, and a maximum deviation of 28° in the torsion angle C(27)–C(28). The only remarkable difference lies in the relative orientation between the planes of the naphthoquinone nucleus and that of the *ansa*-chain, which make an angle of 71° in BRTOL (V) and 97° in CMRS (II).

In conclusion, the low antimicrobial activity found in CMRS (II) does not seem related to the influence, if any, of

Table 6. Distances (Å) of the atoms of CMRS from the best plane through C(1)—C(10)

C(1)	−0.10	C(19)	3.81	C(37)	5.68
C(2)	0.12	C(20)	5.15	C(38)	0.42
C(3)	0.12	C(21)	5.27	C(39)	2.02
C(4)	−0.09	C(22)	6.62	N	0.32
C(5)	−0.03	C(23)	6.70	O(1)	−0.27
C(6)	0.11	C(24)	5.64	O(2)	−0.04
C(7)	0.09	C(25)	5.70	O(3)	0.28
C(8)	−0.03	C(26)	4.52	O(4)	−0.28
C(9)	−0.09	C(27)	4.71	O(5)	1.72
C(10)	−0.10	C(28)	3.57	O(6)	4.85
C(11)	0.01	C(29)	2.69	O(7)	6.90
C(12)	0.38	C(30)	−1.07	O(8)	7.99
C(13)	−0.48	C(31)	5.46	O(9)	6.62
C(14)	−0.21	C(32)	7.81	O(10)	4.97
C(15)	−0.15	C(33)	5.76	O(11)	−0.83
C(16)	0.16	C(34)	3.21	O(12)	−0.10
C(17)	1.38	C(35)	7.95	O(13)	−0.22
C(18)	2.63	C(36)	9.00	O(14)	1.62

Table 7. Distances (Å) between O(1), O(2), O(9), and O(10) in rifamycins

	CMRS (II)	RIFB (III)	RIFMP (IV)
O(1)–O(2)	2.54	2.6	2.48
O(1)–O(9)	7.00	6.7	6.16
O(1)–O(10)	5.76	5.7	5.41
O(2)–O(9)	7.42	7.8	6.82
O(2)–O(10)	7.03	7.5	6.93
O(9)–O(10)	2.73	2.7	2.72

Co-ordinates (Å) of the oxygen atoms O(1), O(2), O(9), and O(10) in rifamycins

	CMRS (II)	RIFB (III)	RIFMP (IV)
O(1)	x = 1.3	1.3	1.3
	y = 2.6	2.8	2.8
	z = −0.3	0.3	0.1
O(2)	x = −1.2	−1.2	−1.2
	y = 2.8	2.8	2.8
	z = 0.1	−0.1	0.2
O(9)	x = 2.4	2.1	2.0
	y = 1.5	0.5	1.7
	z = 6.5	6.5	6.1
O(10)	x = 4.2	4.1	4.0
	y = 2.5	1.7	2.8
	z = 4.7	5.1	4.7

The unitary reference system has the origin in the middle point between C(9) and C(10), the x axis along the C(10)–C(3) direction, the z axis perpendicular to the plane of C(3), C(9), and C(10), and the y axis perpendicular to x and z axes, and oriented along the C(10)–C(9) direction.

the methoxycarbonyl group on the *ansa*-chain conformation, and must therefore be attributed to other factors.[3]

A comparison of the *ansa*-chain chromophore-ring junctions observed in various ansamycins shows that only four kinds of conformers seem to be possible. Among these, three have been already met in the solid state: the situation found in RIFB (III) and RIFMP (IV), that found in CMRS (II) and BRTOL (V), and that found in TOL (VI). Evidence has been provided for the whole set of four possible conformers by the ^{1}H n.m.r. study of CMRS (II), and of its hydroquinone form CMRSV, in various solvents, in which the two compounds display combinations of conformers, in different percentages (Figure 8). In detail, the ^{1}H n.m.r. spectrum of CMRSV in D_2O is attributed to one conformer whose structure resembles the molecular structure found for CMRS (II) and BRTOL (V)

Table 8. Torsion angles (°) along the skeleton of the *ansa*-chain, calculated from solid-state co-ordinates. The convention of Klyne and Prelog [19] has been adopted

	CMRS (II)	RIFB (III)	RIFMP (IV)
C(1)–C(2)–N–C(15)	−141	−32	−55
C(2)–N–C(15)–C(16)	177	180	179
N–C(15)–C(16)–C(17)	63	−43	−31
C(15)–C(16)–C(17)–C(18)	2	5	4
C(16)–C(17)–C(18)–C(19)	169	168	155
C(17)–C(18)–C(19)–C(20)	−179	−175	−165
C(18)–C(19)–C(20)–C(21)	−30	−11	−19
C(19)–C(20)–C(21)–C(22)	180	170	169
C(20)–C(21)–C(22)–C(23)	−178	−179	−176
C(21)–C(22)–C(23)–C(24)	57	53	62
C(22)–C(23)–C(24)–C(25)	−174	174	165
C(23)–C(24)–C(25)–C(26)	169	155	159
C(24)–C(25)–C(26)–C(27)	180	174	153
C(25)–C(26)–C(27)–C(28)	180	−170	−171
C(26)–C(27)–C(28)–C(29)	−110	117	118
C(27)–C(28)–C(29)–O(5)	−176	−168	−175
C(28)–C(29)–O(5)–C(12)	−127	49	65
C(29)–O(5)–C(12)–O(3)	−52	−79	−78

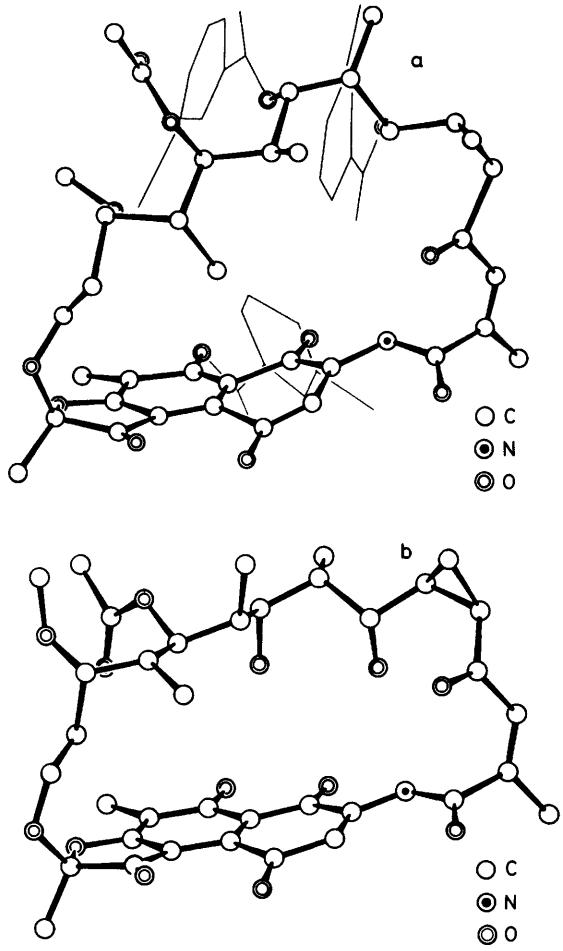

Figure 6. a, Molecular structure of BRTOL (V) (in the same orientation as CMRS in Figure 1). b, Molecular structure of TOL (VI) (in the same orientation as CMRS in Figure 1)

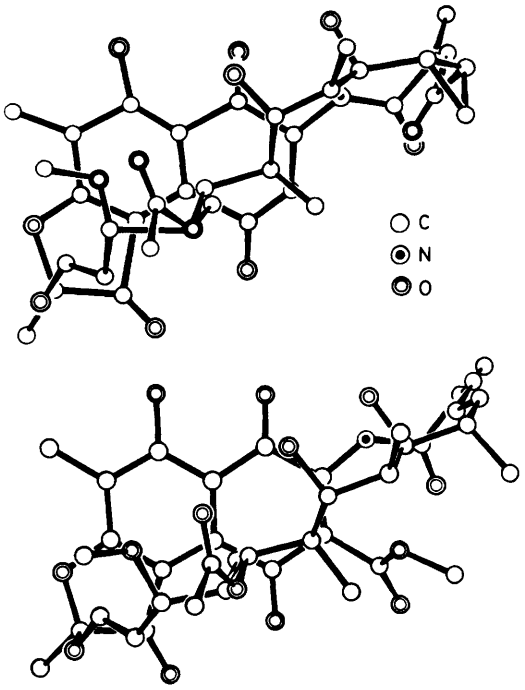

Figure 7. Molecular structures of BRTOL (V) (upper) and CMRS (II) (lower); projections on the plane of the naphthoquinone nucleus. In BRTOL the three bromobenzoate residues are omitted

	A B	A B′	A′ B	A′ B′
Solid state	RIFB RIFMP		TOL	CMRS BRTOL
Solution > majority conformer < minority conformer	CMRS> in $CDCl_3$	CMRS in D_2O	CMRS< in $CDCl_3$	CMRSV in D_2O

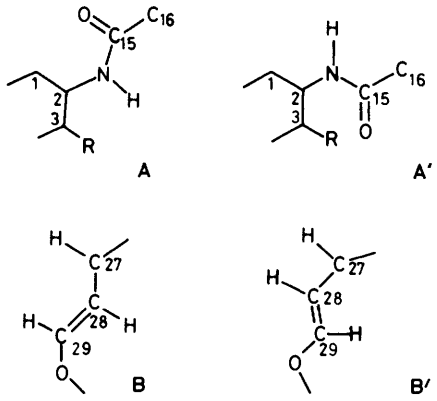

Figure 8. Scheme of the four kinds of possible *ansa*-chain chromophore-ring junctions

in the solid state. The ^1H n.m.r. spectrum of CMRS (II) in $CDCl_3$ is attributed to a mixture of two conformers in a proportion of 3 : 1; the prevalent one displays a molecular conformation similar to those found for RIFB (III) and RIFMP (IV) in the solid state, while the minor conformer has a molecular structure resembling that found for TOL (VI) in the solid state. Finally, the CMRS (II) spectrum in D_2O displays a structure attributed to the only conformer not yet found in the solid state.

As an extension of this research, a systematic study by ^1H n.m.r. of the molecular structures in solution of several derivatives of rifamycins S and SV is being published separately.[14]

Acknowledgements

Technical assistance by Mr. A. Amorese, secretarial help by Mrs. M. Colasuonno, and graphical design by Mr. L. Indrizzi are gratefully acknowledged.

References

1 G. Hartmann, K. O. Honikel, F. Knusel, and J. Nuesch, *Biochim. Biophys. Acta*, 1967, **145**, 843.
2 H. Umezawa, S. Mizuno, K. Yamazaki, and K. Nitta, *J. Antibiot.*, 1968, **21**, 234.
3 M. Brufani, L. Cellai, S. Cerrini, W. Fedeli, A. Segre, and A. Vaciago, *Mol. Pharmacol.*, 1982, **21**, 394.
4 M. Brufani, S. Cerrini, W. Fedeli, and A. Vaciago, *J. Mol. Biol.*, 1974, **87**, 409.
5 M. Gadret, M. Goursolle, J. M. Leger, and J. C. Colleter, *Acta Crystallogr., Sect. B*, 1975, **31**, 1454.
6 K. Kamiya, T. Sugino, Y. Wada, M. Nishikawa, and T. Kishi, *Experientia*, 1969, **25**, 901.
7 M. Brufani, L. Cellai, S. Cerrini, W. Fedeli, and A. Vaciago, *Mol. Pharmacol.*, 1978, **14**, 693.
8 G. Germain, P. Main, and M. M. Woolfson, *Acta Crystallogr., Sect. A*, 1971, **27**, 368.
9 D. W. J. Cruickshank, in ' Computing Methods in Crystallography,' Pergamon, Oxford, 1965, p. 112.
10 ' International Tables for X-Ray Crystallography,' Kynoch Press, Birmingham, 1974, vol. IV, p. 99.
11 J. R. Carruthers and R. Spagna, Abstracts, 7th Italian Crystallographic Association Meeting, Bologna, Italy, 1975, p. 65.
12 S. Cerrini and R. Spagna, Abstracts, 4th European Crystallographic Meeting, Oxford, 1977, p. 7.
13 J. Leitich, W. Oppolzer, and V. Prelog, *Experientia*, 1964, **20**, 343.
14 L. Cellai, S. Cerrini, A. Segre, M. Brufani, W. Fedeli, and A. Vaciago, *J. Org. Chem.*, 1982, **47**, 2652.
15 C. A. Haasnoot, F. A. A. M. De Leeuw, and C. Altona, *Tetrahedron*, 1980, **36**, 2783.
16 A. Segre, L. Zetta, and A. Di Corato, *J. Mol. Spectrosc.*, 1969, **32**, 296.
17 M. F. Dampier, C. W. Chen, and H. W. Whitlock, *J. Am. Chem. Soc.*, 1976, **98**, 7064.
18 A. A. Bothner-By, *Adv. Magn. Reson.*, 1965, **1**, 195.
19 W. Klyne and V. Prelog, *Experientia*, 1960, **16**, 521.
20 S. K. Arora, *Acta Crystallogr., Sect. B*, 1981, **37**, 152.

Received 23rd *October* 1981; *Paper* 1/1644